Subtidal across-shelf velocity structure and surface transport effectiveness on the Alabama shelf of the northeastern Gulf of Mexico

Brian Dzwonkowski,[1] Kyeong Park,[1,2] and Lide Jiang[3,4]

Received 1 April 2011; revised 13 July 2011; accepted 18 July 2011; published 13 October 2011.

[1] A 3.33 year time series of velocity and hydrographic data from a mooring site on the 20 m isobath of the Alabama shelf in the northeastern Gulf of Mexico are used to examine across-shelf circulation. The flow structure and surface transport are determined on this wide shallow shelf system, in which wind stress is a primary forcing mechanism, over a wide range of environmental conditions. The relatively long data set allows the along- and across-shelf wind stress responses to be separated so that their individual contributions to the flow structure can be analyzed. This study finds that both along- and across-shelf wind stress play a role in the across-shelf circulation. While the along-shelf wind is correlated with the currents during all seasons, the across-shelf shelf wind is most clearly correlated with the currents during fall and winter when the water column is least stratified and the across-shelf wind stress is strongest. In addition, wind stress magnitude, mid-depth vertical shear of the horizontal velocity, and stratification all show significant relationships with across-shelf transport effectiveness to varying degrees. The wide range of stratification conditions provides new insight on the influence of stratification on transport effectiveness and across-shelf wind stress forcing. Under very low stratification conditions, there is no apparent relationship between stratification and transport effectiveness, and across-shelf wind stress can generate a significant forcing contribution. As stratification increases, across-shelf wind stress becomes less important and the transport effectiveness increases to a point, above which, there is again no clear relationship with stratification.

Citation: Dzwonkowski, B., K. Park, and L. Jiang (2011), Subtidal across-shelf velocity structure and surface transport effectiveness on the Alabama shelf of the northeastern Gulf of Mexico, *J. Geophys. Res.*, *116*, C10012, doi:10.1029/2011JC007188.

1. Introduction

[2] Transport processes on coastal shelves provide a pathway for mass property and material exchange, which can have a critical impact on the state of a marine system. The consequences of across-shelf transport can be beneficial or deleterious and often result in predominant or seasonal characteristics in a given region. For example, there are a number of regions in which across-shelf surface transport induced upwelling results in some of the most productive oceanic regions of the world [*Lalli and Parsons*, 1997]. In contrast, the offshore advection of relatively fresh, nutrient rich water, as in the case of Mississippi River discharge in the northern Gulf of Mexico, can contribute to the formation of massive hypoxic water masses [e.g., *Wiseman et al.*, 1997; *Rabalais et al.*, 2002].

[3] The understanding of across-shelf circulation on continental shelves lags behind its along-shelf counterpart, and there are a number of questions being actively investigated in regards to across-shelf transport. In wind-driven systems, the most basic explanation typically evokes Ekman dynamics, in which along-shelf wind drives across-shelf advection of surface waters which by continuity requires a subsurface advective return flow. In this idealized view (assuming a small Burger Number), the surface and bottom flows occur in boundary layers. As derived by *Ekman* [1905], the boundary layer depth (δ_E) is represented by $\delta_E = (2A/f)^{1/2}$ where A is a constant vertical eddy viscosity and f is the Coriolis parameter. As commented by *Fewings et al.* [2008], this along-shelf wind driven coastal Ekman circulation is a main mechanism in forcing across-shelf exchange on the middle and outer shelf areas [e.g., *Ekman*, 1905; *Sverdrup*, 1938; *Smith*, 1981]. However, this idealized two layered across-shelf circulation is often complicated

[1]Dauphin Island Sea Lab, Dauphin Island, Alabama, USA.
[2]Department of Marine Sciences, University of South Alabama, Dauphin Island, Alabama, USA.
[3]Center for Satellite Applications and Research, National Environmental Satellite, Data, and Information Service, NOAA, Camp Springs, Maryland, USA.
[4]Cooperative Institute for Research in the Atmosphere, Colorado State University, Fort Collins, Colorado, USA.

0148-0227/11/2011JC007188

by a number of factors that affect the overlapping of the surface and bottom boundary layers and thus, reduce the relative importance of Ekman circulation. The same magnitude of along-shelf wind stress may generate different amounts of across-shelf transport at different locations on the shelf as a result of different levels of boundary layer overlap. The efficiency or effectiveness of along-shelf wind stress in driving across-shelf transport has been shown to decrease with deceasing depth [*Lentz*, 2001; *Kirincich et al.*, 2005]. Deep waters have more space to fully develop the boundary layers, i.e., no overlap, and consequently can be more efficient in using the available along-shelf wind stress energy.

[4] In addition to the absolute depth of the water, other environmental factors can influence the effectiveness of along-shelf wind stress in driving across-shelf transport. Of primary concern are those that may affect the turbulent diffusion of momentum, as parameterized by the vertical eddy viscosity, $A(z)$. The relationships between A and environmental factors are well presented by *Kirincich and Barth* [2009] and only brief comments are provided here. Environmental factors that enhance vertical mixing, such as wind stress, increase the value of A, which in turn increases the boundary layer thickness. Conversely, stratification, which inhibits vertical mixing, decreases the value of A and consequently decreases the boundary layer thickness [*Weisberg et al.*, 2001; *Tilburg*, 2003; *Kirincich et al.*, 2005]. These changes in boundary layer thickness may affect boundary layer overlap and thus can enhance or constrain transport on the inner shelf. In addition, velocity shear, which is often considered in the parameterization of A, is another factor that affects transport on the inner shelf as increased (decreased) velocity shear decreases (increases) the value of A and thus reduces (enhances) boundary layer overlap.

[5] Many studies have linked stratification to the effectiveness of along-shelf wind stress in driving across-shelf transport [e.g., *Allen et al.*, 1995; *Allen and Newberger*, 1996; *Lentz*, 2001; *Weisberg et al.*, 2001; *Austin and Lentz*, 2002; *Tilburg*, 2003; *Kirincich et al.*, 2005; *Liu and Weisberg*, 2007]. Complicating the picture, however, *Kirincich and Barth* [2009] find that, at event time scales (2–7 d), there is not a relationship between transport effectiveness and stratification, but rather transport effectiveness is set by wind stress and eddy viscosity at their study site; transport effectiveness being a measure of how the observed transport compares to the theoretical Ekman transport (see section 2.2). Linking these new findings with previous results from seasonal time scales is not clear-cut, but *Kirincich and Barth* [2009] suggest it is likely related to the short event time scales during their study. It should also be noted that the range of stratification observed in this study is relatively narrow (0.01–0.04 kg m^{-4}) compared to that typically observed in the northern Gulf of Mexico inner shelf, e.g., 0.00–0.54 kg m^{-4} by *Dzwonkowski et al.* [2011, Figure 2f].

[6] Regardless of the factors that impact the effectiveness of along-shelf wind stress, as this forcing function becomes less important, others may play a more important role. As summarized by *Fewings et al.* [2008], several theoretical [*Ekman*, 1905; *Garvine*, 1971; *McCreary et al.*, 1989] and numerical modeling [*Li and Weisberg*, 1999a, 1999b; *Tilburg*, 2003] studies show that across-shelf wind stress can generate across-shelf circulation. Observational efforts, however, typically find across-shelf wind stress to be a secondary player [*Liu and Weisberg*, 2005, 2007], becoming a dominant driver of circulation during strong episodic events [*Trasviña et al.*, 1995; *Liu and Weisberg*, 2005; *Dzwonkowski et al.*, 2009]. However, *Fewings et al.* [2008] find that during small wave conditions, across-shelf wind stress is the dominant driver of the across-shelf circulation at a 12 m deep study site and demonstrate the relative importance of wave forcing, across-shelf wind stress, and along-shelf wind stress with shelf depth, based on theoretically and numerically derived surface layer transport. None of these observational studies, however, have had long-term synoptic-scale density data to accompany the velocity analysis, and we will show in this paper that stratification plays a critical role in determining the relative importance of along- and across-shelf wind stress on the shelf.

[7] Despite the importance of across-shelf transport, little is known of it on the inner and midshelf of Mississippi/Alabama of the United States (Figure 1). Lack of observations in this part of the northeastern Gulf of Mexico is a primary reason for this information gap as there have only been a limited number of studies examining general circulation and hydrographic conditions in this region. The previous observational studies have been based on satellites images [*Schroeder et al.*, 1985; *Abston et al.*, 1987; *Dinnel et al.*, 1990; *Stumpf et al.*, 1993], a near-bottom current meter [*Chuang et al.*, 1982], or surface drifters [*Schroeder et al.*, 1987; *Ohlmann and Niiler*, 2005]. They have found that the shelf current variability is wind driven with limited focus, if any, on across-shelf flow in the study region. Previous modeling studies have been primarily focused on monthly or seasonal currents and attribute the modeled current patterns primarily to regional wind forcing [*Morey et al.*, 2003a, 2003b, 2005; *He and Weisberg*, 2002, 2003; *Smith and Jacobs*, 2005].

[8] A recent study, using in situ current observations from a single long-term ADCP deployment, shows that the depth-averaged seasonal mean across-shelf velocity component is small (<1 cm s^{-1}) and generally directed onshore [*Dzwonkowski and Park*, 2010, Table 1, Figure 3]. However, there is observational and modeling evidence that shows a seasonal freshening on the shelf [*Jochens et al.*, 2002; *Morey et al.*, 2003a; *Dzwonkowski et al.*, 2011] which requires some processes, either surface transport, along-shelf advection, large evaporation-precipitation differences, horizontal mixing in the surface layer or some combination thereof, to account for the observed and modeled freshening. In fact, *Morey et al.* [2003a, 2003b] attribute the seasonal freshening to a shift in the wind stress which would be consistent with a wind-driven Ekman surface boundary layer transporting fresher water offshore of the eastern coast of Louisiana. However, on account of a sharp change in coastline orientation in the Louisiana/Mississippi border, these south winds would be expected to have no effect and possibly work against the offshore transport of the coastal water on the Mississippi/Alabama shelf. This region is of particular interest as it has been recently impacted by the Deepwater Horizon oil spill, but more importantly, it receives large amounts of freshwater from the Mobile Bay

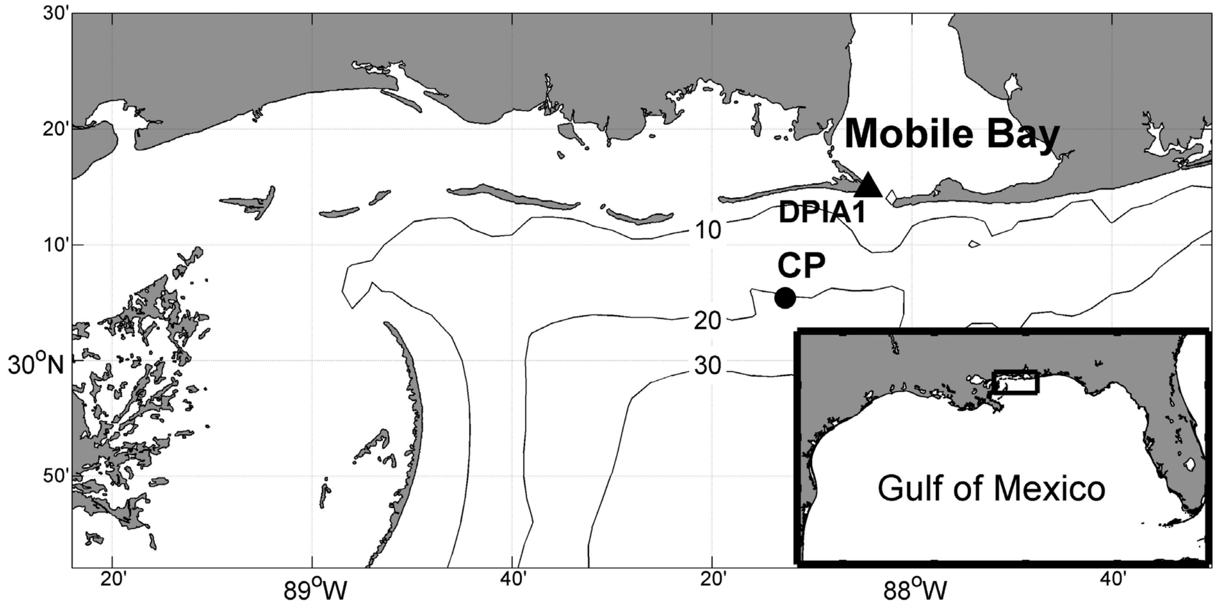

Figure 1. Map of the Alabama shelf and lower Mobile Bay, showing the bathymetry (m), mooring station (CP), and the NOAA National Data Buoy Center station DPIA1 on Dauphin Island (solid triangle).

River system (the fourth largest discharge in the United States), the Pascagoula River, the Pearl River, and Lake Pontchartrain. The impact of these freshwater sources on the Mississippi/Alabama shelf, and in particular, the observed seasonal freshening, remains unclear.

[9] Here, we investigate across-shelf transport processes on the inner Alabama shelf just south of Mobile Bay. Of regional interest is the exploration of the seasonal mean surface transport patterns and the local forcing factors that influence these patterns. In particular, we aim to determine whether surface transport plays a significant role in the transport of the material across the Alabama shelf. Of broader interest, this study examines the vertical structure of the across-shelf component of the current velocity and the resulting across-shelf transport at synoptic time scales over a wide range of wind and freshwater discharge (i.e., stratification) conditions. This study clarifies the relationship between the across-shelf surface transport and the driving mechanisms of the along- and across-shelf wind stress, as well as the modulating influence of wind stress, vertical shear of the horizontal velocity, and stratification, all factors that are expected to impact the vertical turbulent diffusion of horizontal momentum. This study is distinct from the previous work on across-shelf circulation since the relatively long duration of the time series of both velocity and density represents a unique set of observations, which allows for the analysis of the time varying contributions of wind stress components (along- and across-shelf), independent of each other, in conjunction with event-scale fluctuations in stratification. To our knowledge, this is the first work of this kind on the Mississippi/Alabama shelf, a region clearly in need of improved understanding as demonstrated by the Deepwater Horizon oil spill. The data and the analysis methods used are described in section 2, followed by the results of this study in section 3. A discussion is provided in section 4 with a summary and conclusions in section 5.

2. Data and Method

2.1. Data Sources

[10] To analyze the water column current structure and surface transport with their associated forcing mechanisms, velocity and hydrographic time series data, in conjunction with local wind velocity and river discharge were obtained. The velocity and hydrographic data are described in detail by *Dzwonkowski and Park* [2010] and *Dzwonkowski et al.* [2011], respectively. Thus, only limited comments are presented here. The velocity and hydrographic data were collected at a site on the 20 m isobath located approximately 20 km offshore and approximately 25 km west-southwest of the Mobile Bay mouth (station CP in Figure 1). The site was instrumented with an upward-looking ADCP, two SeaBird MicroCats (SBE 37-SMP) at the near-surface (15.7 m above bottom, mab) and bottom (0.2 mab) and 10 SeaBird thermistors (SBE 39) at Δz = 1–1.5 m intervals. The hydrographic sensor deployment began October 2004, followed by the ADCP in November and the data till March 2008 are used in this study. Data from the ADCP were collected at 0.5 m bins between 2 and 19 mab, of which 2–17 mab are consistently reliable. Note that 2 m bins were used during November–December 2004 and then 1 m bins during January–March 2005. All instruments were programmed to record 20 min averages, from which hourly data are derived. The resulting data set includes time series of vertical profiles of current velocity and temperature, and salinity and density at the surface and bottom. The velocity bin at 17 mab and salinity/temperature data at 15.7 mab are referred to as the surface data because the CTD casting data show that this depth is typically in the surface mixed layer, except in the presence of estuarine outflow plumes which can result in

vertical gradients shallower than a depth of 4.3 m [*Dzwonkowski et al.*, 2011]. The instruments were regularly serviced, but intermittent gaps in the data due to biofouling or other instrument malfunctions did arise, some of which are rather large, O(weeks).

[11] The forcing functions of wind velocity and freshwater discharge were obtained from local sources. Hourly wind data during the study period were collected from the NOAA National Data Buoy Center station DPIA1 at Dauphin Island, http://www.ndbc.noaa.gov/to_station.shtml (Figure 1). Daily discharge data for the Mobile River system was obtained at two U.S. Geological Survey's gauging stations for Alabama River (31°32′48″N, 87°30′45″W: USGS 02428400) and Tombigbee River (31°45′25″N, 88°07′30″W: USGS 02469761). Their sum was used as a total freshwater discharge into Mobile Bay, following *Park et al.* [2007].

2.2. Data Processing and Analysis

[12] As this study is primarily focused on subtidal processes, several basic procedures are applied to the hydrographic, current and forcing data. The short data gaps of 12 h or less are filled using linear interpolation. Using the height of the sensor (13.5 m) and the bulk formula of *Large and Pond* [1981], the wind velocity time series are transformed into wind stress at 10 m. Vertical shear ($d\boldsymbol{U}/dz$) is estimated following the procedures of *Garvine* [2004] where $d\boldsymbol{U}/dz$ is calculated from a fifth-order polynomial fit to a vertical profile. Additionally, the magnitude of mid-depth velocity shear is determined by averaging the shear between 5 and 15 mab, equal distance from the surface and bottom boundary. The level of water column stratification ($\Delta\rho/D$) is estimated by dividing the surface and bottom density difference ($\Delta\rho$) by the distance between the two instruments (D), similar to that of *Kirincich and Barth* [2009]. Following this, all time series are low-pass filtered using a 40 h Lanczos filter to remove tidal and near-inertial signals. A depth-averaged current is calculated by integrating the current over the water column using the trapezoidal method. The velocity data not available near the surface and bottom are obtained by assuming a constant value from the upper (lower) most value to the surface (bottom) [*Shearman and Lentz*, 2003]. A linear trend from the upper (lower) value to the surface (bottom) was also performed, however little difference resulted.

[13] As mentioned above, the regional coastline and bathymetry experience a significant change in orientation to the west of the study site (Figure 1). Given the focus of this study on across-shelf transport processes, determining the appropriate along- and across-shelf orientation is important. In a study conducted very close to our study site (25 m isobath south of Dauphin Island), *Chuang et al.* [1982] find that an east/west orientation well represents the along-shelf axis for the local isobaths and coastline offshore of Alabama. More significantly, the principal components of the depth-averaged current at the study site support this coordinate system, having a major axis orientation along the east/west axis (90.9/270.9 axis) and having a relatively rectilinear axis relationship (major axis = 10.2 cm s^{-1} and minor axis = 2.9 cm s^{-1}) as is expected on a shallow continental shelf. Hence, the (u, v) velocity components are used as the along- and across-shelf components, respectively.

[14] To focus on subtidal depth-dependent flow structure, across-shelf transport is calculated by removing the depth-averaged across-shelf velocity, and then integrating it from the first zero crossing to the surface [*Dever*, 1997]:

$$T_s(t) = \int_{\zeta}^{0} [\mathrm{v(z,t) - V(t)}]dz \tag{1}$$

where T_s = across-shelf surface transport; z = depth, ζ = water depth of the first zero crossing; v = across-shelf velocity component; V is the depth-averaged v. When conducting the depth integration in equation (1) using the trapezoidal method, as in the calculation of depth-averaged velocity, the velocity data not available near the surface and bottom are obtained by assuming a constant value from the uppermost value to the surface. The observed surface transport (T_s) is compared with the theoretically derived Ekman transport T_E [*Lentz*, 2001]:

$$T_E(t) = \frac{\tau^{sx}}{\rho f} \tag{2}$$

where τ^{sx} = along-shelf wind stress; ρ = density. From a linear regression of the form $T_s = a \cdot T_E + b$, the slope a provides an estimate of the transport fraction, the fraction of theoretical T_E realized in T_s. The larger the transport fraction, the more "effective" the across-shelf transport.

[15] This study examines the transport effectiveness over seasonal time scales as well as over binned synoptic conditions similar to the approaches of *Lentz* [2001] and *Kirincich and Barth* [2009], respectively. As such, the data are conditionally sampled in a number of ways. At the largest scale in this study, the data are grouped by season using typical definitions for temperate climates of spring (March–May), summer (June–August), fall (September–November), and winter (December–February). To examine relationships during event specific conditions, the data are binned over a range of wind stress, mid-depth velocity shear, and stratification similar to the work of *Kirincich and Barth* [2009]. Over these time scales, basic analysis techniques including correlations, averaging, and transport fraction calculations are performed.

[16] The along- and across-shelf wind stress are significantly correlated at weather band time scales (1.7–15 d) in the study area [*Dzwonkowski et al.*, 2011, Table 2], which complicates the analysis of the effect of the wind stress components. The effect of either the along- or across-shelf wind stress component is examined by conditionally sampling the data during time periods when either component is dominant. This approach is similar in concept to the methodology of *Fewings et al.* [2008]. The directional component is considered dominant if the wind stress vectors fall within a 45° window of the along- or across-shelf axis. Smaller windows are tested, yielding similar values with less statistical confidence because of the reduced data points involved. Similar to the transport calculations, the depth-averaged across-shelf component is removed from the vertical velocity data for these analyses. In addition, lagged conditional analysis is similarly tested with the majority of statistically

Table 1. Seasonal Surface Transport (T_s), Transport Fraction and Vertical Velocity Shear (d$\boldsymbol{U}$/dz)

Season	T_s (m^2 s^{-1}) Mean	T_s (m^2 s^{-1}) SD[a]	Transport Fraction	|d$\boldsymbol{U}$/dz| (cm s^{-1}m^{-1}) Mean	|d$\boldsymbol{U}$/dz| (cm s^{-1}m^{-1}) SD	Percent Data
Spring						
2005	−0.03	0.50	0.60	0.95	1.00	94
2006	−0.08	0.42	0.39	1.57	0.96	74
2007	0.01	0.31	0.29	1.02	0.63	100
Summer						
2005	0.05	0.33	1.08	1.26	0.81	65
2006	−0.01	0.29	1.07	0.90	0.55	100
2007	−0.06	0.35	0.67	1.05	0.61	41
Fall						
2005	0.00	0.26	0.05	0.86	0.66	64
2006	−0.02	0.28	0.19	0.82	0.61	100
2007	−0.01	0.19	0.07	0.62	0.45	100
Winter						
2004	0.00	0.37	0.26	0.95	0.61	81
2005	−0.05	0.41	0.45	1.05	0.72	86
2006	−0.16	0.32	0.25	1.08	0.68	100
2007	0.02	0.38	0.21	0.79	0.60	66

significant values occurring at zero lag and no qualitative difference between those with longer lags. Thus, only the results with the conditional 45° window, zero lag and a 95% confidence significance level (using a minimum decorrelation timescale of 24 h to determine the effective degrees of freedom, EDOF) are presented, unless specifically noted.

3. Results

3.1. Seasonal Mean Conditions and Transport

[17] As a starting point on the nature of across-shelf transport on the Alabama shelf, the seasonal averages and environmental conditions are examined. These seasonal mean values of the surface transport are generally offshore with negative seasonal mean T_s occurring eight out of 13 seasons, but tend to be small with means typically being nearly 0–20% of their standard deviations (Table 1). Despite being small, the seasonal duration (three months) associated with the mean values would result in large volumes of surface transport. There is no clear seasonal pattern in the mean surface transport, but there is some evidence of seasonality in the magnitude of its fluctuations where fall (spring) has the lowest (highest) standard deviations. A clear seasonality exists in the transport fraction which shows high effectiveness during summer/spring and low effectiveness during winter/fall. There is also limited evidence of seasonality in the mid-depth velocity shear with fall having the lowest means and standard deviations of its magnitude. Note that the percent of missing velocity data during each season is provided in Table 1, where velocity data coverage is over 60% in all but one season.

[18] The seasonal averages of the environmental conditions are given in Table 2. For the along-shelf wind stress, the means are westward in all seasons with the weakest mean wind conditions during summer. Whereas the across-shelf wind stress has a seasonal shift from north in fall/winter to south in summer with considerable weakening in the wind stress during summer, being typically less than a third of winter values. Assessing seasonal stratification conditions is challenging with the given data set because of data gaps. However, for seasons where there are high data coverage percents, there is a relationship between discharge and shelf stratification with which the stratification values during periods of limited data appear to be in agreement. Not surprisingly, there are high (low) stratification values in spring and summer (fall and winter) which are associated with high (low) discharge levels and high (low) solar insolation. Despite colder, dryer, and windier conditions in fall and winter, some stratification still persists at the study site.

[19] The seasonal relationships between environmental variability and surface transport are examined through their transport fractions (Figure 2). Conditional sampling would

Table 2. Seasonal Mean Environmental Conditions, Wind Stress (τ^s), Stratification ($\Delta\rho/D$), Discharge (Q_R), and Estimated Seasonal Ekman Depths

Season	Wind Stress τ^s (Pa) Mean τ^{sx}	Wind Stress τ^s (Pa) Mean τ^{sy}	Wind Stress τ^s (Pa) SD[a]	$\Delta\rho/D$ (kg m^{-4}) Mean	$\Delta\rho/D$ (kg m^{-4}) Percent Data[b]	Q_R[c] (m^3 s^{-1})	δ_E[d] (m)
Spring							
2005	−0.008	−0.004	0.037	0.26	71	2758	4
2006	−0.010	0.007	0.048	0.29	20	1962	5
2007	−0.021	−0.003	0.042	0.13	77	561	5
Summer							
2005	−0.018	0.007	0.123	0.33	83	1876	7
2006	−0.005	0.005	0.017	0.23	93	292	3
2007	−0.002	0.007	0.017	0.15	19	207	3
Fall							
2005	−0.019	−0.028	0.065	0.09	7	649	7
2006	−0.014	−0.013	0.042	0.09	45	573	6
2007	−0.024	−0.023	0.038	0.03	72	195	6
Winter							
2004	−0.013	−0.029	0.050	0.14	100	2972	6
2005	−0.005	−0.021	0.042	-	-	1889	-
2006	−0.012	−0.029	0.043	0.09	22	1442	6
2007	−0.016	−0.026	0.046	0.06	64	517	7

[a]SD, standard deviation of the wind stress magnitude.
[b]Data percentage for stratification whereas wind stress and discharge have no data gap.
[c]Discharge value with a 11 d lag, a lag time between the gauge stations and the study site [*Dzwonkowski et al.*, 2011].
[d]Seasonal Ekman depths following those of *Weatherly and Martin* [1978].

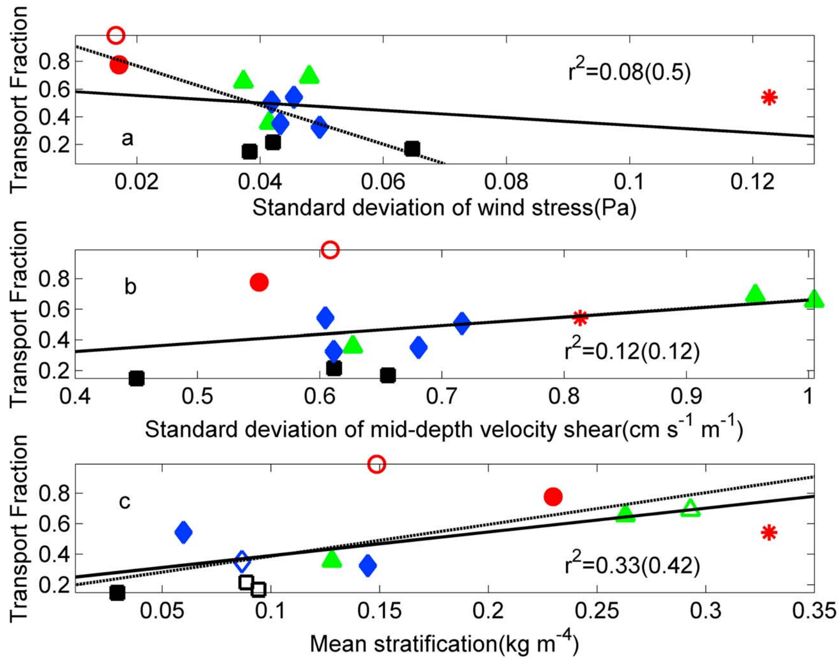

Figure 2. Scatterplots of transport fraction as a function of (a) standard deviation of wind stress magnitude, (b) standard derivation of the mid-depth velocity shear, and (c) mean stratification for seasons of spring (triangle), summer (circle), fall (square), and winter (diamond), with open symbols indicating <60% data coverage. Two linear fits are for all data (solid line) and that with the summer 2005 data (asterisk) removed (dashed line), and the r^2 value in the parenthesis is for the dashed line. See the text for the exclusion of the summer 2005 data. Note that the transport fraction is calculated with no conditional sampling on account of individual seasonal data limitations.

result in a limited number of data for each individual season and seasonal grouping would give only four data points. Either method is data limited for observing trends, so all available data are used in Figure 2. Multiple tropical storms that directly affected the study area result in the unusually large wind stress during summer of 2005, with its standard deviation over 7 times larger than the other summer wind data (Table 2), resulting in a statistically insignificant regression (Figure 2a). With the summer 2005 data excluded, wind stress and stratification show notable, statistically significant trends with the transport fraction having r^2 values of 0.5 and 0.42, respectively (Figure 2). Transport effectiveness decreases with increasing wind stress, but increases with increasing stratification. On seasonal time scales, transport effectiveness shows no statistically significant relationship with vertical velocity shear.

3.2. Synoptic-Scale Variability

[20] Insight into the relative relationships between across-shelf transport and the associated forcing functions can be gained by examining the data at synoptic time scales [*Kirincich and Barth*, 2009]. As such, a brief qualitative description of the representative synoptic-scale patterns and characteristics in the data is provided in this section, reinforced with a quantitative examination in sections 3.3 and 3.4. As an example of the wide range of conditions observed over the study period, the subtidal signals of winter 2007–2008 are presented. During this period, wind stresses typically range between ±0.1 Pa, with larger episodic events, particularly north wind events (Figure 3a). The wind stress components often act in concert with north wind frequently being associated with west winds. Consequently, given that synoptic-scale current variability of the shelf is presumably wind driven, the surface transport response to wind forcing components is not straightforward (Figure 3b). Under the two months of available data during this period (December and February), there are markedly different responses. The overall surface transport fluctuations are smaller in December compared to those in February. The observed T_s is almost entirely accounted for by the theoretical T_E in February whereas the two are quite different in December. In addition, there are events (e.g., 3 and 6 December) when the across-shelf wind stress appears to be driving a weak offshore transport while along-shelf wind stress is weak or unfavorable for offshore transport. There appears to be a marginal, at best, increase in the velocity shear from December to February, with slightly larger peaks occasionally occurring in February (Figure 3d). Yet, there is markedly different stratification (Figure 3e), with much stronger density differences in February that are associated with dramatic increases in river discharge levels (Figure 3f). Note that temperature is almost homogeneous in the vertical during winter (Figure 3g), whereas the vertical temperature gradient is an important contributor to spring and summer stratification in the study area [*Dzwonkowski et al.*, 2011]. An additional point worth noting is that the depth-averaged across-shelf velocity component (Figure 3c), being relatively small (±4 cm s^{-1}), does not appear to be forced by

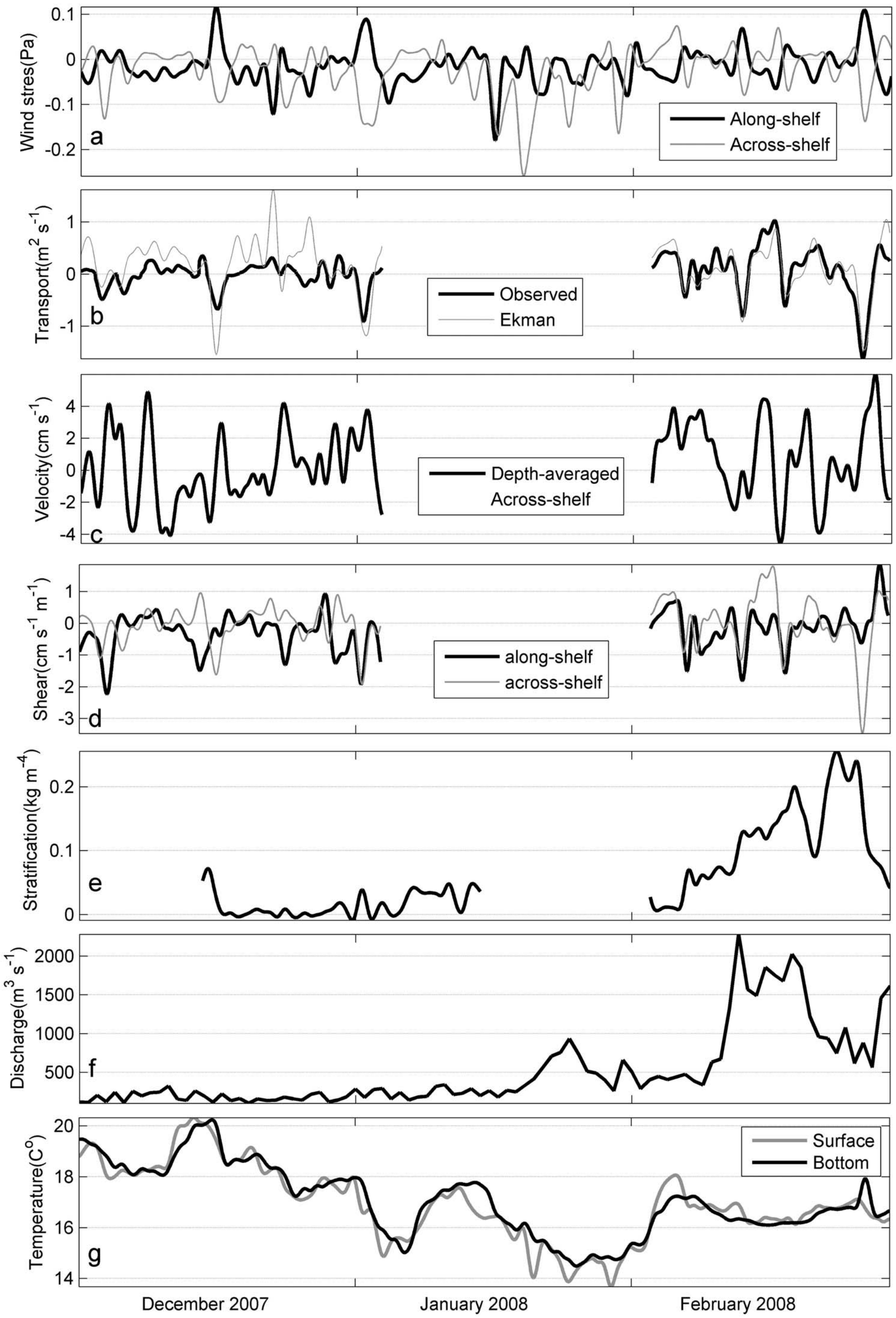

Figure 3. Subtidal time series: (a) along- and across-shelf wind stress, (b) observed and theoretical Ekman across-shelf transport, (c) depth-averaged across-shelf velocity, (d) along- and across-shelf mid-depth velocity shear, (e) stratification, (f) 11 d lagged river discharge from the Mobile Bay watershed, and (g) surface and bottom temperature. The positive (negative) along-shelf wind is west (east) wind, and the positive (negative) across-shelf wind is south (north) wind in Figure 3a. The positive (negative) value is onshore (offshore) in Figures 3b and 3c.

wind stress, consistent with previous studies [e.g., *Lentz*, 2001; *Jiang et al.*, 2010]. For example, the three largest positive velocity peaks in December (4, 10, and 23) do not correspond to peaks in either wind stress component.

3.3. Effect of Wind Stress Components

[21] The varying importance of the wind stress components on the water column structure and hence transport is examined using conditional correlations and averaging

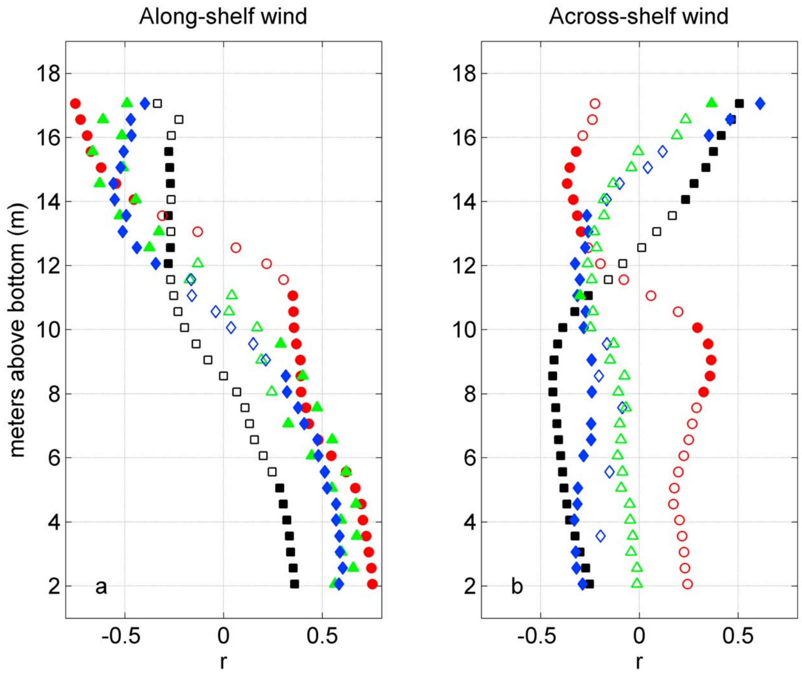

Figure 4. Correlations between the across-shelf velocity component and wind stress for the dominant (a) along-shelf and (b) across-shelf wind conditions during spring (triangle), summer (circle), fall (square), and winter (diamond) with the filled symbols indicating statistically significant correlations. The directional wind component is considered dominant if the wind stress vectors fall within a 45° window of the along- or across-shelf axis. The number of values used in the correlation calculations varies. Note different bin sizes with 2 m bins during winter 2004, 1 m bins during spring 2005, and then 0.5 m bins thereafter.

during time periods when either the along- or across-shelf component is dominant. Both the along- and across-shelf wind stresses are significantly correlated with the across-shelf velocity structure as the results for each season demonstrate a shift in the seasonal importance of the wind stress components (Figure 4). The along-shelf (across-shelf) wind stress has higher correlations in spring/summer (fall/winter). The highest along-shelf wind stress correlation with both the surface and bottom across-shelf currents occurs during summer, a period in which the across-shelf wind stress has no physically meaningful correlations. The along-shelf correlations during spring are slightly smaller compared to summer values, but spring does have a single significant across-shelf wind stress correlation at the uppermost depth, which might indicate transition from significant winter to insignificant summer correlations at the surface (Figure 4b). The highest across-shelf correlations occur during winter, but this season also has significant correlations with along-shelf wind stress having *r* values nearly as high as those in spring. Fall also has high across-shelf wind stress correlations similar to winter values. In terms of along-shelf wind stress, fall has the weakest correlations, but the top three insignificant values are just below the 95% confidence level. Many of the correlations at mid-depths are small and insignificant in accordance with the expectation of the across-shelf current response to wind stress being focused on the surface and bottom layers.

[22] The conditional averaging of the across-shelf velocity under the dominant wind conditions provides insight into the surface transport. Figure 5 shows the mean response of the across-shelf velocity structure to west (upwelling favorable) and east (downwelling favorable) wind dominant conditions for each season as well as the velocity structure normalized by the conditionally averaged wind stress. Not surprisingly, the general response of the water column velocity is similar over all seasons with offshore (onshore) flow at the surface and onshore (offshore) flow at the bottom during west (east) wind conditions, consistent with the theoretical Ekman circulation and the correlations in Figure 4. However, there are several features that should be noted. Under east wind conditions, summer responses have relatively small vertical shear at mid-depth (5–11 mab), separating the surface and bottom boundary layers under both east and west wind conditions. Spring shows this response only for east wind stress. The two most conspicuous details are the asymmetry between the west and east wind response profiles and the event averaging durations. During spring, despite having notably weaker west wind stress, <65% of the east wind stress, the speeds of the surface (bottom) velocities are nearly (over) twice their east wind counterparts. There is a similar disparity in summer and winter. Fall has the weakest response to both west and east wind stress as well as the weakest profile asymmetry, despite having mean wind stress magnitudes similar to those of spring and winter. This asymmetry is clearly shown in the velocity structure normalized by the wind stress (Figures 5c and 5d), which effectively demonstrates the amount of current driven by a unit wind stress is much stronger under west wind conditions near the surface and bottom of the water column. With the exception of summer which has a roughly even duration,

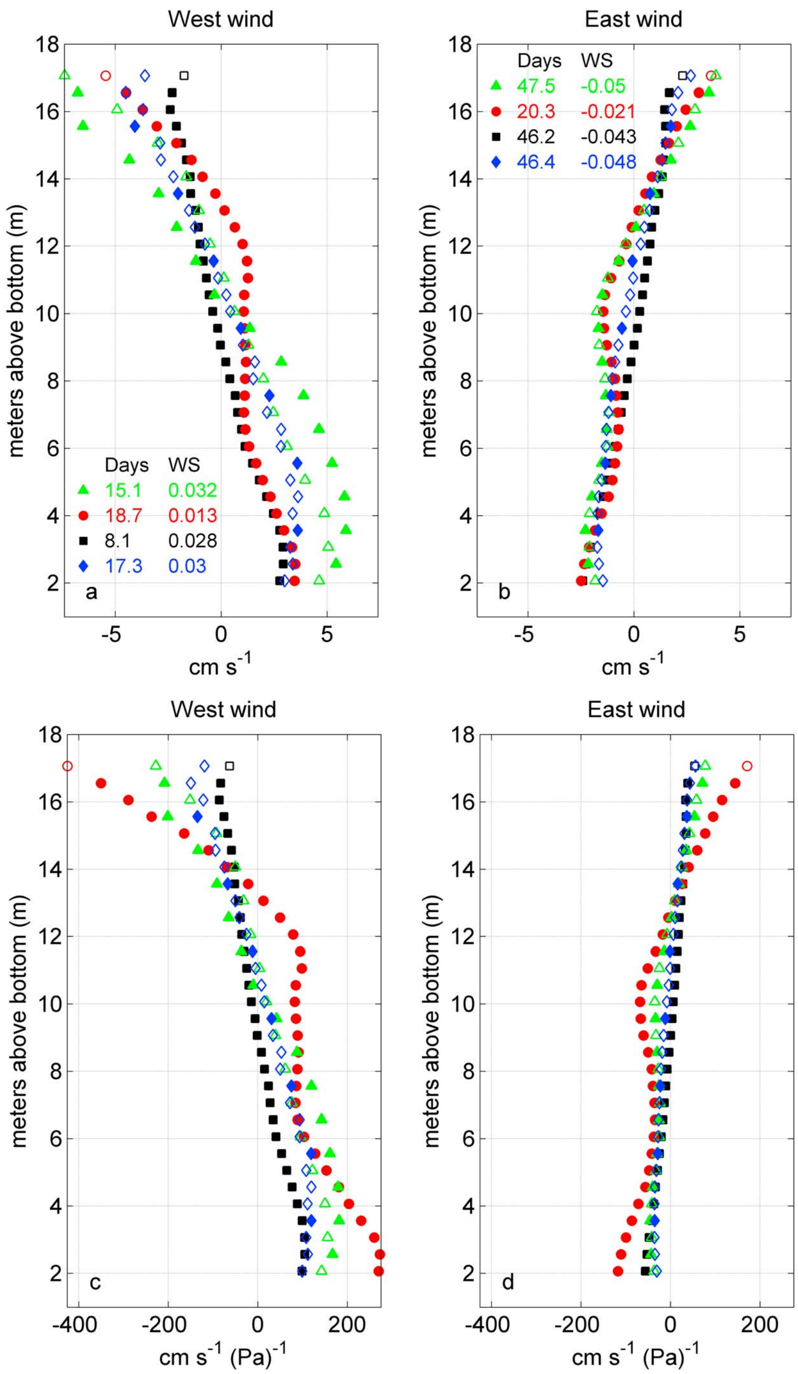

Figure 5. Vertical structure of the across-shelf velocity conditionally averaged during periods of the dominant (a) positive, upwelling favorable and (b) negative, downwelling favorable along-shelf wind stress conditions for spring (triangle), summer (circle), fall (square), and winter (diamond).The positive (negative) velocity is onshore (offshore). The number of data averaged varies, and the longest averaging periods (days) and the corresponding mean wind stress (WS) are given and marked with the filled symbols. (c and d) The velocity normalized by WS. Note different bin sizes with 2 m bins during winter 2004, 1 m bins during spring 2005, and then 0.5 m bins thereafter.

the averaging durations are much longer under east wind conditions.

[23] In regards to the across-shelf wind stress, the across-shelf velocities averaged during south and north wind conditions demonstrate a much less coherent picture (Figure 6). The overall velocity structure is quite different between seasons and wind stress directions, as are the mean wind stress values under which the conditional averaging is conducted. Under the strong wind stress conditions, i.e., north wind during spring, fall, and winter, there is an offshore (onshore) flow at the surface (bottom), and the surface flows are 2 to 3 times stronger than the bottom flows (Figure 6b).

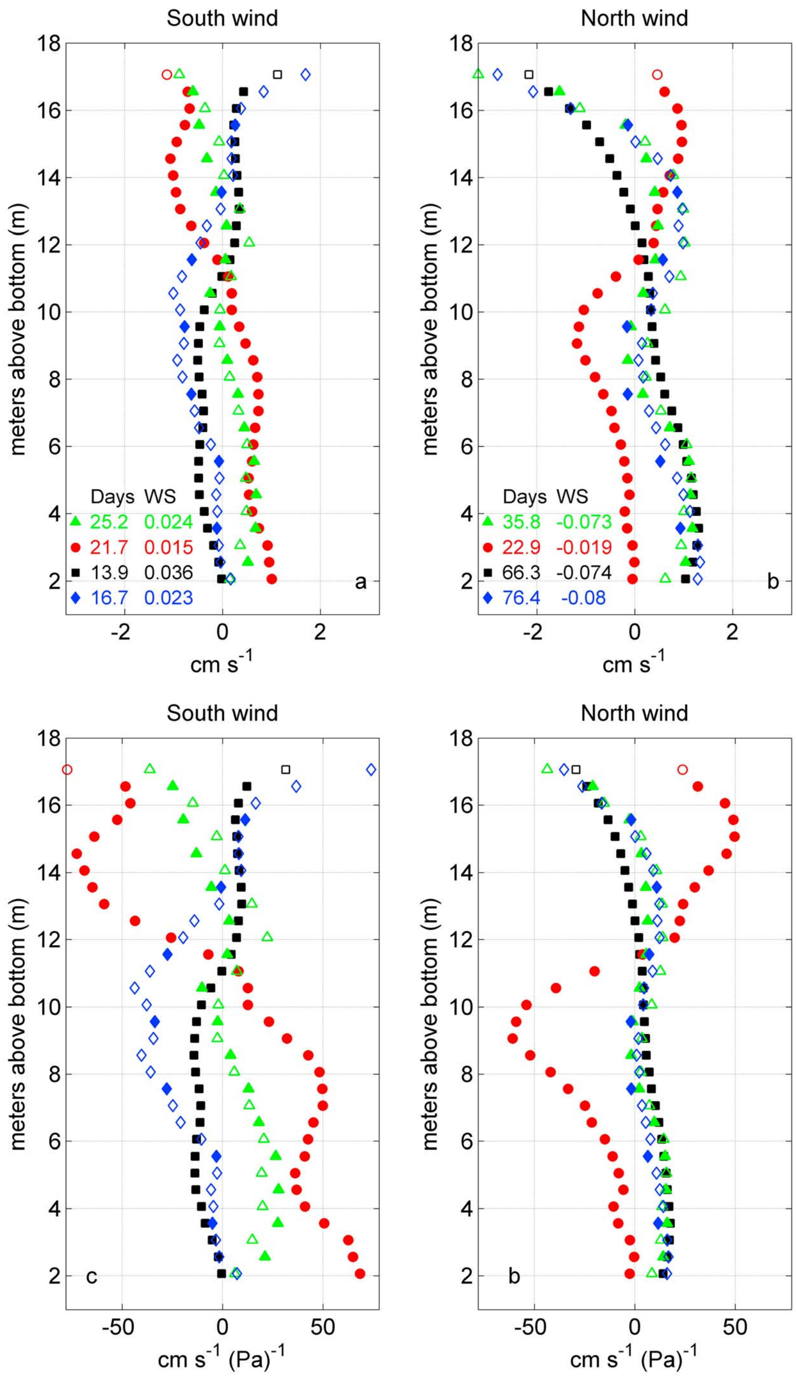

Figure 6. The same as Figure 5 but for the dominant (a) positive, onshore and (b) negative, offshore across-shelf wind stress conditions for spring (triangle),summer (circle), fall (square), and winter (diamond). (c and d) The velocity normalized by WS. Note the reduced range of the *x* axis compared to Figure 5.

Fall is the only season having a simple profile with a single zero crossing, separating the surface offshore flow from the bottom onshore flow. Whereas spring and winter have multiple mid-depth zero crossings. Under south wind conditions, there is no substantial surface flow in all seasons. The bin depths with the longest averaging period (filled symbols in Figure 6a) show currents less than 1 cm s^{-1} with these profiles associated with wind stress values less than half of the north wind stresses. However, the bin depths with shorter averaging periods (open symbols in Figure 6a) at the surface vaguely suggest a very shallow northward flow during winter and fall. The velocity profiles during summer and spring, under south wind conditions, are not associated with the wind forcing, i.e., the surface flow in the opposite direction of the wind stress. The reduced capacity of the across-shelf wind stress in driving flow is clearly shown in the velocity structure normalized by the wind stress (Figures 6c and 6d) which has values that are

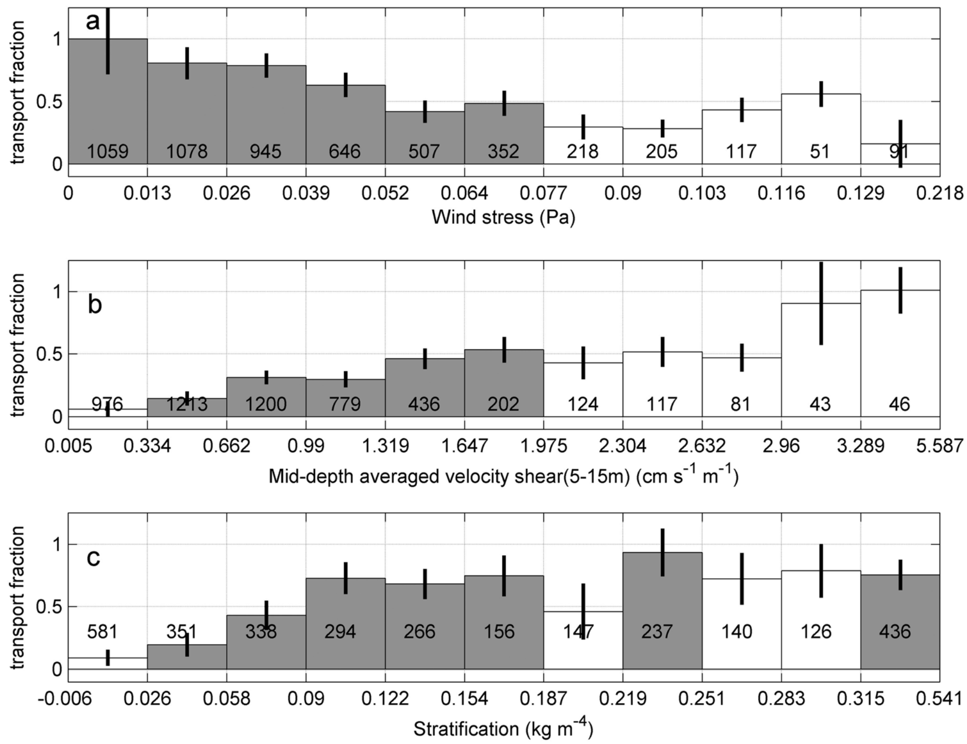

Figure 7. Transport factions calculated using the binned data by levels of (a) wind stress magnitude, (b) mid-depth velocity shear, and (c) stratification. For each bar, an integer indicates the number of data in that bin, a gray color indicates a statistically significant relationship between the measured and theoretical transports, and a vertical line at the top indicates the confidence intervals of the regression.

typically less than half of their along-shelf wind stress counterparts (Figures 5c and 5d) near the surface and bottom of the water column. Overall, the north wind conditions are more frequent, as noted by the longer averaging durations during fall and winter.

3.4. Factors Influencing Transport Effectiveness

[24] As demonstrated by the analysis in section 3.3, surface across-shelf velocity structure is related to wind stress, however its relative effectiveness in driving transport can be influenced by a number of factors, of which, this study examines wind stress magnitude, mid-depth vertical shear of the horizontal velocity, and stratification. The relationships between these parameters and their associated transport fraction are examined by binning the conditionally sampled data over event specific values during the study period. Seasonally grouping the data show qualitatively similar patterns to the total data set, but the various ranges of the seasonal environmental data and more importantly, the limited data number in the seasonal groupings leads to noisy results, often lacking statistical confidence when compared to the total data set. Thus, only the results from the conditionally sampled total data set are presented.

[25] The relationships between parameters and their associated transport fractions for 10 evenly spaced bins and an eleventh adjustable bin to accommodate extreme values are shown in Figure 7. The correlation coefficients for the statistically significant relationships range from 0.36 to 0.83, with 15 (out of 18) larger than 0.5. The general trends, where there are statistically significant results, show that transport effectiveness at synoptic scales decreases with increasing wind stress magnitude and increases with increasing velocity shear and stratification. Even with higher levels of wind stress not being statistically significant, there are hints of the general pattern of decreasing transport effectiveness with increasing wind strength. Whereas the stratification begins to generally level off at higher levels, of which several bins are significant (the sixth, eighth, and eleventh bins). Also the first bin in both velocity shear and stratification (i.e., the lowest levels) is not significant despite a modest number of values (i.e., over 10 EDOF).

4. Discussion

4.1. Relationships Between Seasonal Transport and Wind Stress

[26] This shelf system is historically considered wind driven at the synoptic time scales, and this study supports this notion. Removing the depth-averaged component of the across-shelf velocity (nonwind driven component) allows this study to emphasize the contribution of the wind-driven processes to the across-shelf velocity structure and surface transport. The seasonal mean along-shelf wind conditions (Table 2) would be expected to drive onshore surface Ekman transport of the order of 0.1 m^2 s^{-1}. However, the assumptions required for idealized Ekman transport are not met, and the disparity between the observed and theoretical transport is notable in that the observed transport (Table 1) is typically directed offshore or at least an order of magnitude below the estimated onshore Ekman transport. The

results of this study provide some insight into these apparently conflicting results. First, the strong asymmetry in the response to the along-shelf wind stress allows west wind stress to be more effective at transporting surface water offshore during all seasons, particularly in spring and summer when the asymmetry is strongest (Figure 5). Second, the across-shelf north wind becomes an important forcing mechanism in the surface layer during spring, fall, and winter (Figure 6b), although it is not as effective as the along-shelf wind stress in driving transport. Note the reduced x-axis range in Figure 6 compared to Figure 5, despite strong north wind stress nearly 2 times larger than the along-shelf wind stress. However, the prominence of north wind stress during fall and winter with O(0.02–0.03 Pa) in Table 2 and the reduced effectiveness of downwelling wind stress likely compensates for the mean east wind occurring during these seasons. Other factors that may contribute to the mean offshore surface transport are discussed in section 4.3.

4.2. Implications for the Wind Stress Forced Current Response

[27] The study site responds to along-shelf wind stress in a manner consistent with coastal Ekman circulation, that is, along-shelf wind drives onshore (offshore) flow in the surface layer and offshore (onshore) flow in the bottom layer during east (west) wind events. However, the synoptic response to along-shelf wind stress varies notably from season to season. During summer, and to a lesser degree spring, with relatively strong stratification and weak wind stress (Table 2), the expectation is for the surface and bottom boundary layers to have minimal interactions, thus resulting in enhanced Ekman transport. As such, the velocity profiles appear to have distinct boundary layers, separated by a zone of minimum velocity shear (Figures 5a and 5b), and consequently have the highest correlations (i.e., highest r values at surface and bottom in Figure 4a) and the strongest magnitude response to wind stress (i.e., highest current speed per unit mean wind stress in Figures 5c and 5d). Whereas during fall with relatively weak stratification and strong wind stress (Table 2), the expectation is for the surface and bottom boundary layers to be interacting/overlapping, thus resulting in reduced Ekman transport. As such, fall shows the weakest correlations (Figure 4a) and nearly the weakest magnitude response to along-shelf wind stress (Figures 5c and 5d).

[28] These results are qualitatively consistent with the simple first-order Ekman boundary layer estimates for the seasonal conditions. Following *Lentz* [1992], the formula of *Weatherly and Martin* [1978] is used to estimate the surface Ekman depth under stratified conditions (δ_E):

$$\delta_E = 1.3q_*/\sqrt{fN} \tag{3}$$

where q_* is the friction velocity $(\tau_s/\rho)^{1/2}$, f is the Coriolis parameter and N is the buoyancy frequency. The results (Table 2) using the seasonal standard deviation of the wind stress and the mean stratification show that the shallowest (deepest) depths occur during spring/summer (fall/winter): note that the 2005 summer was atypical because of multiple tropical storms. On the basis of the estimate by *Mitchum and Clarke* [1986] that boundary layer overlap begins at $3\delta_E$, the results in Table 2 suggest that the water depth at our study site (20 m) can support separate surface and bottom boundary layers during spring/summer. Whereas it is very likely to have interacting/overlapping boundary layers during fall/winter, it should be noted that across-shelf velocity profiles during the along-shelf wind dominant conditions for spring and summer (Figure 5) suggest somewhat deeper boundary layers than the estimated ones. This is consistent with the findings of *Houghton* [1995] that the *Weatherly and Martin* formula often underestimates the height of boundary layers. Another note of caution comes from the study by *Garvine* [2004], which raises questions about the validity of *Weatherly and Martin*'s estimate in regions under the influence of buoyancy driven coastal currents.

[29] The expected boundary layer interactions also generate temporal variations in the importance of the across-shelf wind stress, which shows the highest (lowest) correlations (Figure 4b) and the strongest (weakest) magnitude response during fall (summer) (Figure 6). This finding is consistent with the response of the hydrographic data to wind forcing; *Dzwonkowski et al.* [2011] find changes in surface temperature and salinity are most correlated with north wind stress directions during late fall and winter. It is worth noting that the range of depth values (approximately 10–30 m for a water column of constant density) for which across-shelf wind stress is expected to be dominant [*Fewings et al.*, 2008, Figure 15] appears to be overly wide for strongly stratified water column. The depth of 20 m locates our study site squarely in the center of the above range, yet our results show that along-shelf wind stress is the more dominant driving mechanism, with higher correlations and stronger across-shelf velocities under equal wind conditions, during the majority of the study period. While the "inner" shelf is expected to have overlapping boundary layers limiting the importance of along-shelf wind stress, the presence of strong stratification at our study site reduces boundary layer interaction, which effectively positions the site outside the "inner" shelf where along-shelf winds are expect to be the dominant player in the across-shelf transport.

[30] As noted in several previous studies [e.g., *Weatherly and Martin*, 1978; *Trowbridge and Lentz*, 1991; *Liu and Weisberg*, 2007], there is an asymmetric response to the along-shelf wind stress (Figure 5). Given the geometry of the shelf slope and the expected slope of isopycnals [*Morey et al.*, 2003a; *Dzwonkowski et al.*, 2011], their ratio is expected to be O(1) during spring and summer. Thus, the observed asymmetry is consistent with the findings of *Weisberg et al.* [2001] and the additional scaling arguments of *Garvine* [2004], whose explanations are derived from the thermal wind effect where buoyancy forcing increases or decreases with the changes in isopycnal slopes that either act in concert with (against) the pressure gradient in the bottom boundary layer during upwelling (downwelling) events. Furthermore, the seasonal evolution of the asymmetry reflects changes that are supported by this explanation with spring and summer (fall and winter) having stronger (weaker) stratification and thus a stronger (weaker) asymmetric response. In terms of the response to the across-shelf wind stress, this asymmetry is not expected to play a major role on account of the thermal wind effect not playing a major role in the flow response; that is, the across-shelf wind stress is relatively important during mixed conditions at the

study site. However, this study is limited by the fact that only relatively weak south winds are observed during the study period, which are too weak to drive significant onshore flow at this site and are typically much weaker than their north wind counterparts.

4.3. Implications for Surface Transport

[31] In terms of transport and transport effectiveness, a similar trend in the relationship between the environmental conditions and the transport fraction is observed, regardless of the means of comparison (Figures 2 and 7). The observed relationships can be interpreted through their assumed effect on vertical eddy viscosity and the consequent impact on the boundary layer extent and thus the surface transport. In general, as wind stress increases, water column turbulence and hence vertical eddy viscosity will increase. Then, the boundary layer depths will increase, enhancing interaction/overlapping of the surface and bottom boundary layers and consequently reducing the transport fraction, as observed in both the seasonal (Figure 2a) and the binned (Figure 7a) data. In terms of vertical velocity shear, as eddy viscosity increases, momentum will be transferred more easily through the water column, thus resulting in a more uniform flow structure, i.e., less velocity shear. Hence, increased shear will decrease eddy viscosity, reducing boundary layer interaction/overlapping and consequently enhancing the transport fraction. This trend is shown in the binned data (Figure 7b), but is not present in the seasonal data (Figure 2b), which suggests that seasonal values of the vertical shear are less important than synoptic variability. Similarly, stratification will decrease the eddy viscosity, reducing the boundary layer extent and enhancing the transport fraction. Increasing the transport fraction with increasing stratification levels is observed in both the seasonal (Figure 2c) and the binned (Figure 7c) data.

[32] Our results are consistent with previous studies in that the seasonal transport fractions are related to stratification [*Lentz*, 2001; *Kirincich et al.*, 2005] and that the binned data are affected by wind stress and velocity shear [*Kirincich and Barth*, 2009]. However, *Kirincich and Barth* [2009, Figure 9] observe across-shelf exchange efficiencies at synoptic scales are only controlled by wind stress and eddy viscosity with no effect from stratification. This differs from our observations (Figure 7). They attribute the lack of importance of stratification to the rapid nature of the fluctuations observed, with typical event time scales of about 30 (40) h for downwelling (upwelling). These time scales are shorter than those observed in this study with seasonally averaged downwelling (upwelling) time scales ranging between 63 and 142 (30–90) h. Additionally, and probably more importantly, the observed range of stratification by *Kirincich and Barth* [2009] (0–0.04 kg m^{-4}) is much narrower compared to that of this study (0–0.5 kg m^{-4}). Examining a subset of our data that is consistent with the range of *Kirincich and Barth* [2009] demonstrates the lack of trend for stratification. In Figure 7c, the first bin is not statistically significant, despite a reasonable number of observations (n = 581). Subdividing this bin data into 4–6 bins yields no trend, consistent with *Kirincich and Barth* [2009, Figure 9c], and none of these bins are statistically significant. This consistency adds confidence to the findings of *Kirincich and Barth* [2009] that, at low-stratification levels, wind stress and velocity shear set the eddy viscosity and hence exchange effectiveness. The results of our study provide additional information that as stratification increases, its role in setting the eddy viscosity enhances; note a dramatic increase in transport fraction from approximately 0.2 to 0.7 as stratification increases from 0.026 to 0.122 kg m^{-4} in the second to the fourth bins in Figure 7c. It is interesting to note that at increasingly higher levels of stratification, there is a leveling of transport effectiveness with statistically significant transport fractions ranging from 0.7 to 0.9. Clearly, this relationship for stratification, as well as the interactions between the environmental factors requires further work.

4.4. Data Limitations

[33] Given the limitations of the data set, there are several issues that this study is unable to address. One of the primary issues arises from the proximity of the study site to the mouth of Mobile Bay. Previous studies based on satellite imagery [*Abston et al.*, 1987; *Dinnel et al.*, 1990] show that the surface extent of the plume can reach the study site. As such, it is not clear to what extent, if any, that plume dynamics affect the flow structure and across-shelf transport. Using satellite imagery and limited in situ salinity data of a single event, *Stumpf et al.* [1993] show that at moderate distances from the Mobile Bay mouth (10–15 km), the plume is very shallow (<2 m deep) and rapidly responses to wind forcing with limited Ekman drift from which it is suggested that the strong shallow pycnocline may limit vertical momentum transfer. The shallow nature of these plume events make them difficult to observe given the limitations of an ADCP, either upward or downward looking. Furthermore, interactions between the Mobile Bay plume and the shelf water have the potential for the development of three dimensional flow features, which cannot be addressed using the data from a single site. Direct interaction with the plume will be limited to only relatively large discharge events, most likely to occur during spring in this study region.

[34] Another limitation of this study results from the inability to address the forcings associated with the across-shelf mean flow. As shown by *Dzwonkowski and Park* [2010], the seasonal mean depth-averaged across-shelf flows are typically small (<1 cm s^{-1}) and of the order of the standard error for the measurement. On synoptic time scales, the fluctuations in the depth-averaged across-shelf flow (Figure 3c) can contribute to short-term across-shelf transport. However, the ability to determine the physical forcing is limited, at best. The seasonal time series show no meaningful relationship with the stress (Figure 3a). Because of this study being based on data from a single site, other processes such as along-shelf divergence, along-shelf pressure gradient, or submesoscale eddies, cannot be assessed.

[35] Additional concerns arise from the regional coastline geography. As can be seen in Figure 1, the 20 and 30 m isobaths have a 90° shift in direction on account of the Louisiana coastline. Both *Chuang et al.* [1982] and *Schroeder et al.* [1985] point out that the wind-driven sea level setup (i.e., along-shelf pressure gradient) associated with this geographic corner may play a dynamical role at

synoptic time scales, although a formal analysis has not yet been conducted.

[36] Other limitations of this study include a lack of wave and wind stress data at the mooring site. Recent studies by *Lentz et al.* [2008] and *Fewings et al.* [2008] show that wave forcing is an important contributor to across-shelf flow structure at shallow sites off of the U.S. east coast. While concurrent wave data is not available at the study site, the wave forcing is expected to be small since the study site is approximately 20 km from shore. Wind stress is determined using the data from a site approximately 20 km shoreward of the study site (Figure 1). This could affect our results in two ways. First, any increase in the wind stress magnitude farther offshore will result in increased Ekman transport values which in turn would reduce transport fraction values. This, however, will not result in qualitative changes of the results. Second, this potential wind stress increase would generate wind stress curl, which is associated with Ekman pumping, the effect of which would be included in the observed transport T_s. A basin-wide study in the Gulf of Mexico show seasonal wind stress curl values ranging from 0 to $-0.5 \cdot 10^{-9}$ Pa cm^{-1} over the Alabama shelf [*de Velasco and Winant*, 1996]. Given the limited observations in the northeastern gulf, it is not clear how representative these values are for the Alabama shelf, but these results do suggest that the effect of wind stress curl is very limited. Additionally, the study site being at approximate 30°N latitude, the resonant latitude for near-inertial motion driven by sea breeze, the summer vertical mixing would be expected to be enhanced as demonstrated by *Zhang et al.* [2010]. The net effect of this process will be captured by the subtidal change in the stratification, but a more detailed examination of this process on mixing and the vertical eddy viscosity is left for future investigations.

5. Summary and Conclusions

[37] This study explores the across-shelf circulation on the Alabama shelf, a region of the U.S. coastal waters for which there is little knowledge of the physical processes. The heavy use of this region by the numerous commercial interests (gas industry, shipping, fisheries, etc.) and the potential for disastrous events, as demonstrated by the recent Deepwater Horizon oil spill, necessitate a better understanding of the regional flow structure and transport processes. This study examines 3.3 years of velocity and hydrographic data from a mooring on the 20 m isobath approximately 20 km offshore of the coastline. The relatively long time series make this study unique in that the data allows for the analysis of the time varying contributions of wind stress components (along- and across-shelf), independent of each other, in conjunction with event-scale fluctuations in stratification. This site is particularly interesting on account of the fact that it receives large quantities of discharge from regional fresh water sources, hence experiences a wide range of stratification levels, which proves critical in assessing the importance of stratification at synoptic time scales. Consequently, this study provides new information about the local circulation as well as more general insight into forcing and response relationships on wide shallow shelves affected by large river discharge.

[38] In terms of the regional circulation, this study finds the surface transport to be primarily offshore despite the predominant downwelling (and thus onshore transport) favorable east wind. To address this conflict, the along- and across-shelf wind stress forcing responses are separated through conditional sampling of the long-term time series. Both along- and across-shelf wind stresses contribute to the observed offshore surface transport and vertical across-shelf velocity structure. The along-shelf wind stress drives a response consistent with coastal Ekman dynamics, i.e., oppositely directed surface and bottom boundary layers, observed during all seasons. During spring and summer, the flow structure shows a stronger asymmetric response, favoring upwelling conditions, that generates the observed offshore surface transport. Fall and winter months have relatively higher (lower) correlations with across-shelf (along-shelf) wind stress. While the typical across-shelf wind stress response is weaker compared to the along-shelf response, the frequency and magnitude of north winds during fall and winter, in conjunction with the reduced effectiveness of along-shelf downwelling wind stress, results in the observed offshore transport during these seasons. These findings are particularly interesting as they suggest other regions with predominately downwelling wind conditions can still support net offshore transport in the surface layer.

[39] More importantly, these seasonal modulations in the relative importance of the forcing/response relationships (i.e., current response to the along and across-shelf wind stress) are consistent with the expected boundary layer behavior (i.e., thicker boundary layer during periods of higher eddy viscosity). This is further demonstrated by examining the transport effectiveness associated with the observed variability in three environmental parameters that are expected to influence vertical eddy viscosity: wind stress, velocity shear, and stratification. Using transport fraction as a metric of effectiveness, conditionally sampled data are compared to seasonal and binned levels of these environmental variables. Transport effectiveness generally increases with decreasing wind stress magnitude, increasing velocity shear, and increasing stratification.

[40] The wide range of observed stratification provides significant new insight into two aspects of this study. First, it demonstrates that the region over which the across-shelf wind stress is expected to dominate the across-shelf flow is severely restricted by stratification. On the basis of the arguments of *Fewings et al.* [2008] which assume mixed conditions, the 20 m site should be dominated by the across-shelf wind driven circulation. However, the across-shelf flow is more highly correlated with the along-shelf wind stress during spring, summer and winter. Even during fall, when the across-shelf flow is better correlated with across-shelf wind stress, the flow magnitude response to the across-shelf wind stress still remains weaker than that of the along-shelf wind stress response. Thus, even under the low-stratification conditions of fall, the across-shelf wind stress response is not a more efficient driver of coastal circulation at this site. Second, it puts the previous work on the transport effectiveness in a broader context. The results of this study agree with those of *Kirincich and Barth* [2009] which found that under low values of stratification the eddy viscosity is controlled by the velocity shear and wind stress magnitude. However, the observations over a boarder

range of stratification does show that stratification plays an important role in determining transport effectiveness, i.e., increasing transport fraction with increasing stratification, likely through modulating eddy viscosity. Furthermore, this data set also suggests that at very high levels above approximately 0.154 kg m^{-4}, there is again no clear relationship between transport faction and stratification. Thus, while the relative importance of these factors is complex and requires additional study, stratification does appear to play a role in the synoptic-scale effectiveness of along-shelf wind-driven transport.

[41] **Acknowledgments.** This work would not have been possible without the collecting and archiving of the data by the Tech Support Group at the Dauphin Island Sea Lab, including Kyle Weis, Roxanne Robertson, Alan Gunter, Mike Dardeau, and Laura Linn. We would like to thank the two reviewers for their helpful comments that enhanced the manuscript. This work was supported by the Fisheries Oceanography in Coastal Alabama funded by Alabama Department of Conservation and Natural Resources–Marine Resources Division and the BP–Gulf of Mexico Research Initiative (GRI) Rapid Response. Finally, we thank Rich Pawlowicz at the University of British Columbia for the freely available MATLAB m_map toolbox which we have found to be useful in our analysis of geophysical data.

References

Abston, J. R., S. P. Dinnel, W. W. Schroeder, A. W. Shultz, and W. J. Wiseman Jr. (1987), Coastal sediment plume morphology and its relationship to environmental forcing: Main Pass, Mobile Bay, Alabama, in *Coastal Sediments '87*, vol. II, edited by N. C. Kraus, pp. 1989–2005, Am. Soc. of Civ. Eng., New York.

Allen, J. S., and P. A. Newberger (1996), Downwelling circulation on the Oregon continental shelf. Part I: Response to idealized forcing, *J. Phys. Oceanogr.*, *26*, 2011–2035, doi:10.1175/1520-0485(1996)026<2011:DCOTOC>2.0.CO;2.

Allen, J. S., P. A. Newberger, and J. Federiuk (1995), Upwelling circulation on the Oregon continental shelf. Part I: Response to idealized forcing, *J. Phys. Oceanogr.*, *25*, 1843–1866, doi:10.1175/1520-0485(1995)025<1843:UCOTOC>2.0.CO;2.

Austin, J. A., and S. J. Lentz (2002), The inner response to wind-driven upwelling and downwelling, *J. Phys. Oceanogr.*, *32*, 2171–2193, doi:10.1175/1520-0485(2002)032<2171:TISRTW>2.0.CO;2.

Chuang, W., W. W. Schroeder, and W. J. Wiseman Jr. (1982), Summer current observations off the Alabama coast, *Contrib. Mar. Sci.*, *25*, 121–131.

de Velasco, G. G., and C. D. Winant (1996), Seasonal patterns of wind stress and wind stress curl over the Gulf of Mexico, *J. Geophys. Res.*, *101*, 18,127–18,140, doi:10.1029/96JC01442.

Dever, E. P. (1997), Wind-forced cross-shelf circulation on the Northern California shelf, *J. Phys. Oceanogr.*, *27*, 1566–1580, doi:10.1175/1520-0485(1997)027<1566:WFCSCO>2.0.CO;2.

Dinnel, S. P., W. W. Schroeder, and W. J. Wiseman Jr. (1990), Estuarine-shelf exchange using Landsat images of discharge plumes, *J. Coastal Res.*, *6*, 789–799.

Dzwonkowski, B., and K. Park (2010), Influence of wind stress and discharge on the mean and seasonal currents on the Alabama shelf of the northeastern Gulf of Mexico, *J. Geophys. Res.*, *115*, C12052, doi:10.1029/2010JC006449.

Dzwonkowski, B., J. T. Kohut, and X. Y. Yan (2009), Seasonal differences in wind-driven across-shelf forcing and response relationships in the shelf surface layer of the central Mid-Atlantic Bight, *J. Geophys. Res.*, *114*, C08018, doi:10.1029/2008JC004888.

Dzwonkowski, B., K. Park, H. K. Ha, W. M. Graham, F. J. Hernandez, and S. P. Powers (2011), Hydrographic variability on a coastal shelf directly influenced by estuarine outflow, *Cont. Shelf Res.*, *31*, 939–950, doi:10.1016/j.csr.2011.03.001.

Ekman, V. W. (1905), On the influence of the Earth's rotation on ocean currents, *Ark. Mat. Astron. Fys.*, *2*, 1–53.

Fewings, M., S. J. Lentz, and J. Fredericks (2008), Observations of cross-shelf flow driven by cross-shelf winds on the inner continental shelf, *J. Phys. Oceanogr.*, *38*, 2358–2378, doi:10.1175/2008JPO3990.1.

Garvine, R. W. (1971), A simple model of coastal upwelling dynamics, *J. Phys. Oceanogr.*, *1*, 169–179, doi:10.1175/1520-0485(1971)001<0169:ASMOCU>2.0.CO;2.

Garvine, R. W. (2004), The vertical structure and subtidal dynamics of the inner shelf off New Jersey, *J. Mar. Res.*, *62*, 337–371, doi:10.1357/0022240041446182.

He, R., and R. H. Weisberg (2002), West Florida shelf circulation and temperature budget for the 1999 spring transition, *Cont. Shelf Res.*, *22*, 719–748, doi:10.1016/S0278-4343(01)00085-1.

He, R., and R. H. Weisberg (2003), West Florida shelf circulation and temperature budget for the 1998 fall transition, *Cont. Shelf Res.*, *23*, 777–800, doi:10.1016/S0278-4343(03)00028-1.

Houghton, R. W. (1995), The bottom boundary layer structure in the vicinity of the Middle Atlantic Bight shelfbreak front, *Cont. Shelf Res.*, *15*, 1173–1194, doi:10.1016/0278-4343(94)00073-V.

Jiang, L., L. C. Breaker, and X.-H. Yan (2010), A model for estimating cross-shore surface transport with application to the New Jersey Shelf, *J. Geophys. Res.*, *115*, C04017, doi:10.1029/2009JC005998.

Jochens, A. E., S. F. DiMarco, W. D. Nowlin Jr., R. O. Reid, and M. C. Kennicutt II (2002), Northeastern Gulf of Mexico Chemical Oceanography and Hydrography Study: Synthesis Report, *OCS study MMS 2002-055*, U.S. Dep. of the Inter., Miner. Manage. Serv., New Orleans, La.

Kirincich, A. R., and J. A. Barth (2009), Time-varying across-shelf Ekman transport and vertical eddy viscosity on the inner shelf, *J. Phys. Oceanogr.*, *39*, 602–620, doi:10.1175/2008JPO3969.1.

Kirincich, A. R., J. A. Barth, B. A. Grantham, B. A. Menge, and J. Lubchenco (2005), Wind-driven inner-shelf circulation off central Oregon during summer, *J. Geophys. Res.*, *110*, C10S03, doi:10.1029/2004JC002611.

Lalli, C. M., and T. R. Parsons (1997), *Biological Oceanography: An Introduction*, 2nd ed., Butterworth-Heinemann, Oxford, U. K.

Large, W. G., and S. Pond (1981), Open ocean momentum flux measurements in moderate to strong winds, *J. Phys. Oceanogr.*, *11*, 324–336, doi:10.1175/1520-0485(1981)011<0324:OOMFMI>2.0.CO;2.

Lentz, S. J. (1992), The surface boundary layer in coastal upwelling regions, *J. Phys. Oceanogr.*, *22*, 1517–1539, doi:10.1175/1520-0485(1992)022<1517:TSBLIC>2.0.CO;2.

Lentz, S. J. (2001), The influence of stratification on the wind-driven cross-shelf circulation over the North Carolina shelf, *J. Phys. Oceanogr.*, *31*, 2749–2760, doi:10.1175/1520-0485(2001)031<2749:TIOSOT>2.0.CO;2.

Lentz, S. J., M. Fewings, P. Howd, J. Fredericks, and K. Hathaway (2008), Observations and a model of undertow over the inner continental shelf, *J. Phys. Oceanogr.*, *38*, 2341–2357, doi:10.1175/2008JPO3986.1.

Li, Z., and R. H. Weisberg (1999a), West Florida shelf response to upwelling favorable wind forcing: Kinematics, *J. Geophys. Res.*, *104*, 13,507–13,527, doi:10.1029/1999JC900073.

Li, Z., and R. H. Weisberg (1999b), West Florida continental shelf response to upwelling favorable wind forcing, 2. Dynamics, *J. Geophys. Res.*, *104*, 23,427–23,442, doi:10.1029/1999JC900205.

Liu, Y., and R. H. Weisberg (2005), Momentum balance diagnoses for the West Florida Shelf, *Cont. Shelf Res.*, *25*, 2054–2074, doi:10.1016/j.csr.2005.03.004.

Liu, Y., and R. H. Weisberg (2007), Ocean currents and sea surface heights estimated across the West Florida Shelf, *J. Phys. Oceanogr.*, *37*, 1697–1713, doi:10.1175/JPO3083.1.

McCreary, J. P., H. S. Lee, and D. B. Enfield (1989), The response of the coastal ocean to strong offshore winds: With application to circulations in the Gulfs of Tehuantepec and Papagayo, *J. Mar. Res.*, *47*, 81–109, doi:10.1357/002224089785076343.

Mitchum, G. T., and A. J. Clarke (1986), The frictional nearshore response to forcing by synoptic scale winds, *J. Phys. Oceanogr.*, *16*, 934–946, doi:10.1175/1520-0485(1986)016<0934:TFNRTF>2.0.CO;2.

Morey, S. L., P. J. Martin, J. J. O'Brien, A. A. Wallcraft, and J. Zavala-Hidalgo (2003a), Export pathways for river discharged fresh water in the northern Gulf of Mexico, *J. Geophys. Res.*, *108*(C10), 3303, doi:10.1029/2002JC001674.

Morey, S. L., W. W. Schroeder, J. J. O'Brien, and J. Zavala-Hidalgo (2003b), The annual cycle of riverine influence in the eastern Gulf of Mexico basin, *Geophys. Res. Lett.*, *30*(16), 1867, doi:10.1029/2003GL017348.

Morey, S. L., J. Zavala-Hidalgo, and J. J. O'Brien (2005), The seasonal variability of continental shelf circulation in the northern and western Gulf of Mexico from a high-resolution numerical model, in *Circulation of the Gulf of Mexico: Observations and Models*, *Geophys. Monogr. Ser.*, vol. 161, edited by W. Sturges and A. Lugo-Fernandez, pp. 203–218, AGU, Washington, D. C.

Ohlmann, J. C., and P. P. Niiler (2005), Circulation over the continental shelf in the northern Gulf of Mexico, *Prog. Oceanogr.*, *64*, 45–81, doi:10.1016/j.pocean.2005.02.001.

Park, K., C.-K. Kim, and W. W. Schroeder (2007), Temporal variability in summertime bottom hypoxia in shallow areas of Mobile Bay, Alabama, *Estuaries Coasts*, *30*, 54–65.

Rabalais, N. N., R. E. Turner, and W. J. Wiseman Jr. (2002), Gulf of Mexico Hypoxia, a.k.a. "The Dead Zone," *Annu. Rev. Ecol. Syst.*, *33*, 235–263, doi:10.1146/annurev.ecolsys.33.010802.150513.

Schroeder, W. W., O. K. Huh, L. J. Rouse Jr., and W. J. Wiseman Jr. (1985), Satellite observations of the circulation east of the Mississippi Delta: Cold-air outbreak conditions, *Remote Sens. Environ.*, *18*, 49–58, doi:10.1016/0034-4257(85)90037-9.

Schroeder, W. W., S. P. Dinnel, W. J. Wiseman Jr., and W. J. Merrell Jr. (1987), Circulation patterns inferred from the movement of detached buoys in the eastern Gulf of Mexico, *Cont. Shelf Res.*, *7*, 883–894, doi:10.1016/0278-4343(87)90004-5.

Shearman, R. K., and S. J. Lentz (2003), Dynamics of mean and subtidal flow on the New England shelf, *J. Geophys. Res.*, *108*(C8), 3281, doi:10.1029/2002JC001417.

Smith, R. L. (1981), A comparison of the structure and variability of the flow field in three coastal upwelling regions: Oregon, Northwest Africa, and Peru, in *Coastal Upwelling*, edited by F. A. Richards, pp. 107–118, AGU, Washington, D. C.

Smith, S. R., and G. A. Jacobs (2005), Seasonal circulation fields in the northern Gulf of Mexico calculated by assimilating current meter, shipboard ADCP, and drifter data simultaneously with the shallow water equations, *Cont. Shelf Res.*, *25*, 157–183, doi:10.1016/j.csr.2004.09.010.

Stumpf, R. P., G. Gelfenbaum, and J. R. Pennock (1993), Wind and tidal forcing of a buoyant plume, Mobile Bay, Alabama, *Cont. Shelf Res.*, *13*, 1281–1301, doi:10.1016/0278-4343(93)90053-Z.

Sverdrup, H. U. (1938), On the process of upwelling, *J. Mar. Res.*, *1*, 155–164.

Tilburg, C. E. (2003), Across-shelf transport on a continental shelf: Do across-shelf winds matter?, *J. Phys. Oceanogr.*, *33*, 2675–2688, doi:10.1175/1520-0485(2003)033<2675:ATOACS>2.0.CO;2.

Trasviña, A., E. D. Barton, J. Brown, H. S. Velez, P. M. Kosro, and R. L. Smith (1995), Offshore wind forcing in the Gulf of Tehuantepec, Mexico: The asymmetric circulation, *J. Geophys. Res.*, *100*, 20,649–20,663, doi:10.1029/95JC01283.

Trowbridge, J. H., and S. J. Lentz (1991), Asymmetric behavior of an oceanic boundary layer above a sloping bottom, *J. Phys. Oceanogr.*, *21*, 1171–1185, doi:10.1175/1520-0485(1991)021<1171:ABOAOB>2.0.CO;2.

Weatherly, G. L., and P. J. Martin (1978), On the structure and dynamics of the oceanic bottom boundary layer, *J. Phys. Oceanogr.*, *8*, 557–570, doi:10.1175/1520-0485(1978)008<0557:OTSADO>2.0.CO;2.

Weisberg, R. H., Z. Li, and F. E. Muller-Karger (2001), West Florida shelf response to local wind forcing: April 1998, *J. Geophys. Res.*, *106*, 31,239–31,262, doi:10.1029/2000JC000529.

Wiseman, W. J., N. N. Rabalais, R. E. Turner, S. P. Dinnel, and A. MacNaughton (1997), Seasonal and interannual variability within the Louisiana coastal current: Stratification and hypoxia, *J. Mar. Syst.*, *12*, 237–248, doi:10.1016/S0924-7963(96)00100-5.

Zhang, X., D. C. Smith IV, S. F. DiMarco, and R. D. Hetland (2010), A numerical study of a sea-breeze-driven ocean Poincare wave propagation and mixing near the critical latitude, *J. Phys. Oceanogr.*, *40*, 48–66, doi:10.1175/2009JPO4216.1.

B. Dzwonkowski and K. Park, Dauphin Island Sea Lab, 101 Bienville Blvd., Dauphin Island, AL 36528, USA. (briandz@disl.org)

L. Jiang, Center for Satellite Applications and Research, National Environmental Satellite, Data, and Information Service, NOAA, 5200 Auth Rd., Camp Springs, MD 20746, USA.